A Multispectral Photoacoustic Imaging Approach to Detect Nerve Injury During Surgery

Manik Kakkar^{1*}, Mohammed Shahid^{2*}, Shri Prabha Shivram¹, Rachana Suresh², William Padovano², Sami Tuffaha², Muyinatu A. Lediju Bell^{1,3,4}

¹Department of Electrical and Computer Engineering, Johns Hopkins University, Baltimore, MD
²Department of Plastic and Reconstructive Surgery, Johns Hopkins School of Medicine, Baltimore, MD
³Department of Biomedical Engineering, Johns Hopkins University, Baltimore, MD
⁴Department of Computer Science, Johns Hopkins University, Baltimore, MD
*These authors contributed equally.

Abstract—Accurate intraoperative assessment of peripheral nerve injury is critical to optimizing surgical decisions and improving patient outcomes, yet current diagnostic tools provide limited specificity to differentiate among uninjured, injured, and regenerating nerve tissue. This paper investigates the feasibility of multispectral photoacoustic imaging to distinguish the absence, presence, and/or severity of nerve injury using ex vivo nerve samples from two swine. Ulnar and median nerves were subjected to one of three conditions: (1) uninjured, (2) transected (injured), or (3) immediate repair following transection (regenerating). These conditions were confirmed through histopathologic analysis using toluidine blue staining. Photoacoustic images were acquired over a 1200-2000 nm wavelength range. Representative photoacoustic spectra revealed distinct spectral signatures among the three nerve states, particularly in the 1240-1300 nm and 1350-1700 nm ranges. Injured and regenerating nerves exhibited greater absorption amplitudes than uninjured nerves across the noted wavelength ranges, indicating changes in tissue composition during nerve injury and repair. These results demonstrate the feasibility of multispectral photoacoustic imaging as a real-time method to identify nerve injury and regeneration, enabling future intraoperative assessment and surgical guidance.

Index Terms—photoacoustic, multispectral, nerve injury, nerve regeneration, intraoperative imaging, swine model, surgical guidance

I. INTRODUCTION

Peripheral nerve injuries affect millions of individuals worldwide typically as a result of trauma or iatrogenic causes [1], [2]. These injuries have the potential to lead to chronic motor dysfunction, sensory deficits, pain, and substantial reductions in quality of life [3], [4]. Following peripheral nerve injury, Wallerian degeneration occurs — a process by which the distal segment of a severed nerve undergoes axonal and myelin breakdown within days after a transection injury. During this process, macrophage infiltration and Schwann cell proliferation also occur, which clear debris and create a regenerative environment. For some injuries, regeneration can then proceed, beginning approximately 1 week post-injury with axonal sprouting and remyelination from the proximal stump and guided outgrowth through the distal nerve sheath. Conservative management without surgical repair may be favored for such regenerating nerves [5]–[8].

Nerves that cannot regenerate require repair (e.g., primary neurorrhaphy, nerve/tendon transfers, nerve grafts). In addi-

tion, identifying healthy nerve donors for grafts or transfers is a critical component of nerve reconstruction. Existing diagnostic modalities, such as electromyography, nerve conduction studies, and intraoperative nerve stimulation, offer limited spatial resolution and specificity, particularly in anatomically complex surgical fields [9], [10].

To address these limitations, ultrasound and magnetic resonance imaging (MRI) could be viewed as potential solutions for preoperative nerve localization [11]–[13]. High-frequency ultrasound offers excellent spatial resolution for visualizing nerves in real-time and is widely used intraoperatively [11]. However, the diagnostic utility of ultrasound is often limited by modest soft tissue contrast, making it difficult to assess the nerve condition [14]. While MRI offers superior soft tissue contrast for preoperative nerve localization, it is impractical for intraoperative use due to cost, accessibility, and long acquisition times [12], [13].

Purely optical techniques (e.g., near-infrared fluorescence, diffuse reflectance spectroscopy) offer the potential to provide biochemical information, but they often require contrast agents and suffer from shallow depth penetration [15], [16]. In contrast, photoacoustic imaging offers a hybrid solution by combining the optical sensitivity to molecular composition with the spatial resolution and depth of ultrasound [17]. Photoacoustic imaging technique leverages the endogenous absorption properties of chromophores such as hemoglobin, lipids, water, and collagen to generate real-time, label-free images of tissue and demonstrated potential for nerve visualization [7], [8], [18], [19].

Myelinated peripheral nerves are rich in lipid content due to their myelin sheaths, which exhibit distinct optical absorption peaks in the near-infrared (NIR) range, particularly near 1210 nm and 1725 nm [20], [21]. Multispectral photoacoustic imaging exploits these spectral features by acquiring data across a continuum of wavelengths to generate amplitude spectra reflective of biochemical composition of chromophores. Prior work validated photoacoustic imaging as a method to differentiate nerves from surrounding muscle, tendon, and vasculature [22], [23]. Our group additionally identified a characteristic lipid absorption peak at 1725 nm specific to nerve tissue, distinct from other lipids such as fat or cholesterol, and



Fig. 1. Experimental setup for multispectral photoacoustic imaging. A nerve sample was embedded in agarose and imaged using a 57 MHz ultrasound transducer coupled to an optical fiber bundle for 1200-2000 nm light delivery.

confirmed this finding through spectrophotometry and *in vivo* photoacoustic measurements of the same nerves [8].

In this paper, we investigate multispectral photoacoustic imaging as a novel technique to detect and characterize peripheral nerve injury and regeneration. We identify unique spectral signatures associated with changes in myelination that occur during Wallerian degeneration and regeneration. Our purpose is to differentiate among injured, regenerating, and uninjured nerves to guide intraoperative surgical decisions.

II. METHODS

A. Swine Nerve Injury Model

A swine model of median nerve injury was utilized. Two 16-week-old Yorkshire x Landrace swine (Oak Hill Genetics, Abbeville, SC) underwent median nerve transection, with Swine 1 undergoing immediate repair. To minimize spontaneous regeneration, the median nerve of the second swine was left unrepaired, and its proximal and distal stumps were diverted into the pectoralis major and biceps brachii muscles, respectively. Nerve samples were harvested 4 and 8 weeks after injury from Swine 1 and 2, respectively. The following samples were acquired for photoacoustic imaging and histopathology: (i) two uninjured ulnar nerves, (ii) one uninjured median nerve, (iii) one median nerve 4 weeks posttransection with immediate repair, and (iv) two median nerves 8 weeks post-transection without repair. These procedures were conducted in accordance with institutional guidelines, with approval from the Animal Care and Use Committee at Johns Hopkins University School of Medicine (Protocol SW23M91).

B. Histopathology & Imaging

Following harvest, a 0.5 cm segment of each nerve was fixed in 4% Formaldehyde and 3% glutaraldehyde in 0.1M phosphate buffer for 48 hours. The samples were then dehydrated through a graded ethanol series, embedded in Epon resin, and cut to obtain 1-2 micrometer cross-sections. We stained the

sections with 1% toluidine blue in 1% sodium borate at 60° C. Light microscopy was performed at $100 \times$ magnification.

Each remaining nerve sample that was not fixed for histopathology was embedded in a 3% w/v agarose phantom immediately after excision, to perform multispectral photoacoustic imaging, employing a VevoLAZR-X system (FUJI-FILM VisualSonics Inc., Toronto, ON, Canada) with a 57 MHz transducer coupled to a fiber bundle for light delivery. The imaging setup consisted of a custom 3D printed holder that secured the ultrasound transducer to the agarose phantom, as shown in Fig. 1. Photoacoustic images were acquired using the laser excitation wavelength range 1200 to 2000 nm, in 5 nm increments, which required approximately 3 minutes per nerve assessment.

III. RESULTS & DISCUSSION

Fig. 2 shows representative histologic images that highlight the distinct morphological differences for each injury condition, consistent with our surgical model. The uninjured

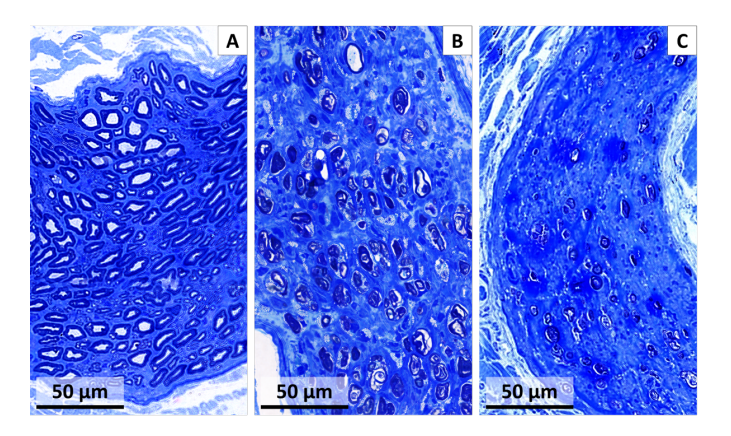


Fig. 2. Representative histology of peripheral nerve samples. (A) Uninjured ulnar nerve with densely packed, myelinated axons and well-organized fascicular architecture. (B) Regenerating median nerve 4 weeks post-transection with immediate repair shows decreased axon density, variable myelination and disruption of normal architecture. (C) Injured median nerve 8 weeks post-transection without repair with marked axonal loss with clearance of most myelin debris.

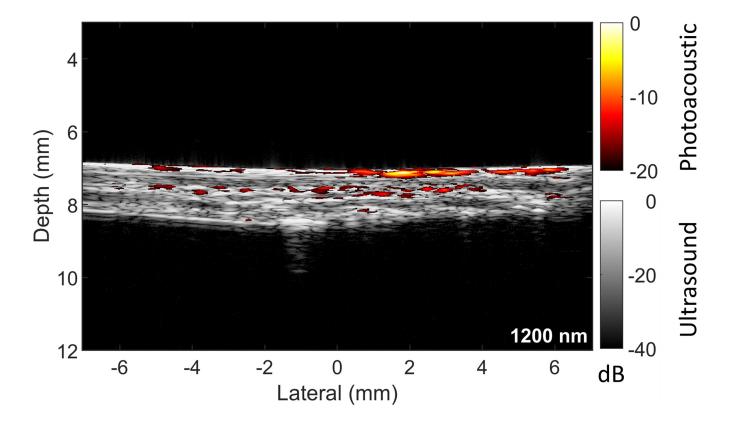


Fig. 3. Representative B-mode ultrasound and photoacoustic overlay image of an *ex vivo*, uninjured swine median nerve. The photoacoustic signals were acquired with 1200 nm wavelength.

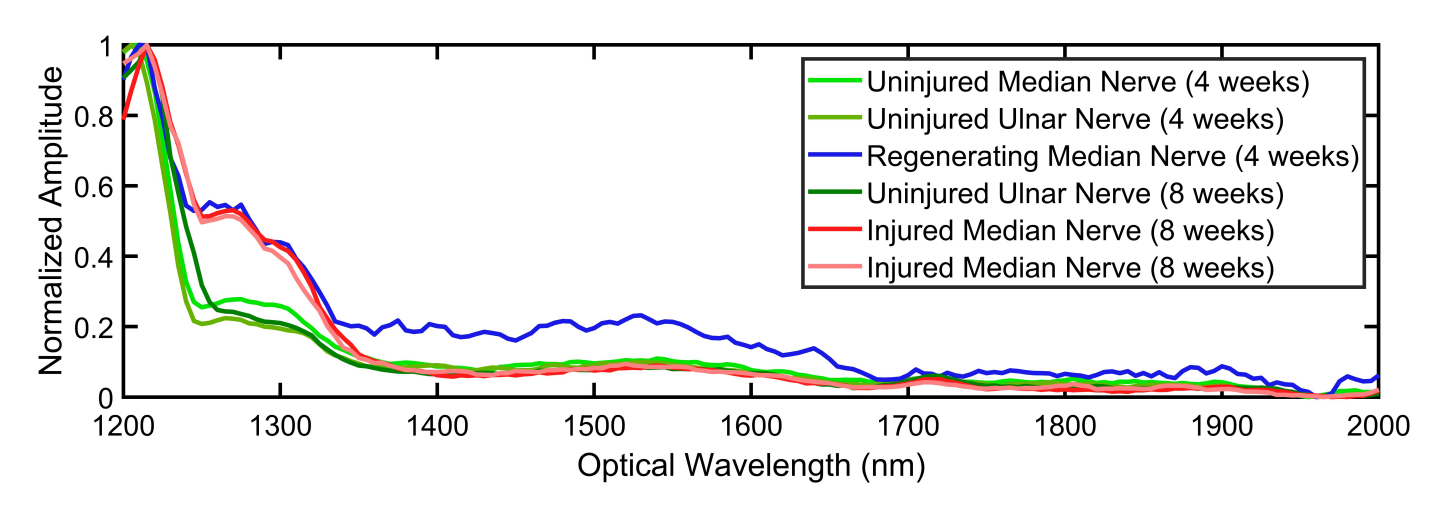


Fig. 4. Normalized photoacoustic amplitude spectra of *ex vivo* peripheral nerve samples from two swine imaged at 4 and 8 weeks post-surgery. Nerves were classified as uninjured (median and ulnar, n=3), regenerating (median, n=1), or injured (median, n=2) and were embedded in 3% w/v agarose and illuminated with wavelengths from 1200 to 2000 nm in 5 nm increments. Spectral differences are evident among nerve conditions, particularly in the 1240–1300 nm and 1350–1700 nm ranges.

nerve samples (Fig. 2A) exhibits densely packed and relatively uniformly sized, myelinated axons arranged within well-organized fascicles, consistent with normal nerve architecture. In contrast, the median nerve harvested 4 weeks after transection and immediate repair shows a reduction in axon density and significant myelin degradation, along with disruption of the fascicular structure (Fig. 2B). These features are consistent with early regenerative changes following nerve injury. In the median nerve samples acquired 8 weeks post-transection without repair (Fig. 2C), profound axonal loss is observed, with only sparse residual fibers visible. In addition, there was near-complete clearance of myelin debris, consistent with advanced Wallerian degeneration and absence of any evidence of regeneration [24].

Fig. 3 shows a representative co-registered photoacoustic and ultrasound image of an uninjured median nerve sample embedded in an agarose phantom. The photoacoustic signals, generated using a 1200 nm laser excitation, are displayed in red and overlaid on the grayscale B-mode ultrasound image. The signals are localized within the boundaries of the nerve, confirming the ability to selectively visualize nerve tissue based on its endogenous optical absorption properties via photoacoustic imaging.

Fig. 4 shows the photoacoustic spectra obtained with the swine nerves described in Section II-A. There are distinct spectral profiles for uninjured, injured, and regenerating nerves. Across the 6 samples, an initial peak near 1210–1220 nm was observed, consistent with the known lipid absorption corresponding to the second overtone of C-H bonds in the NIR-II window [21]. In the 1240–1300 nm wavelength range, injured and regenerating median nerves exhibit higher amplitudes (i.e., 0.4–0.6) compared to uninjured nerves (i.e., 0.2–0.3), indicating increased optical absorption likely due to altered lipid and water content following injury or repair. In the 1350–1700 nm wavelength range, the regenerating nerve maintains elevated amplitudes (~0.2–0.3) relative to both

uninjured and injured nerves (i.e., < 0.1). Spectral flattening in the 1700–2000 nm range is observed across the 6 samples, although the regenerating nerve retains a slightly elevated profile. The increased photoacoustic amplitudes observed with injured and regenerating nerves, relative to the uninjured nerves, may reflect physiological changes that occur during Wallerian degeneration, followed by regeneration. These physiological changes include the clearance of myelin debris and changes in axonal density noted in our histopathologic analysis.

Overall, our results demonstrate the feasibility of using multispectral photoacoustic imaging to differentiate among uninjured, injured, and regenerating nerves, which has implications for intraoperative assessments of nerve viability. As our study focuses on fresh ex vivo nerves, results do not include additional potential contributions from blood perfusion or the influence of other endogenous chromophores present in the in vivo complex tissue environment. Therefore, future work will focus on validating these findings in an in vivo model to assess the effects of the complexity of the surrounding tissue and blood perfusion on the spectral signatures. Classification algorithms may also be devoloped in the future to provide surgeons with real-time, objective feedback. Hence, the work herein provides the necessary foundation to advance the translation of multispectral photoacoustic imaging technology into a tool for surgical decision making, contributing to improved outcomes in nerve repair procedures.

IV. CONCLUSION

This paper is the first to demonstrate the feasibility of using multispectral photoacoustic imaging to differentiate between uninjured, injured, and regenerating peripheral nerves. Nervespecific spectral features were identified from *ex vivo* swine nerve samples, with injured and regenerating nerves exhibiting elevated photoacoustic amplitudes in the 1240–1300 nm and 1350–1700 nm wavelength ranges, relative to uninjured nerves. These spectral windows are particularly promising

because they show consistent separation of photoacoustic signals among the three nerve conditions, providing foundational evidence that photoacoustic imaging may serve as a non-invasive intraoperative tool to identify nerve injury and evaluate regeneration.

ACKNOWLEDGMENT

This work was supported by a TEDCO Maryland Innovation Initiative Technology Assessment Award and a Johns Hopkins Discovery Award.

REFERENCES

- [1] P. Ciaramitaro, M. Mondelli, F. Logullo, S. Grimaldi, B. Battiston, A. Sard, C. Scarinzi, G. Migliaretti, G. Faccani, D. Cocito, et al., "Traumatic peripheral nerve injuries: epidemiological findings, neuropathic pain and quality of life in 158 patients," Journal of the Peripheral Nervous System, vol. 15, no. 2, pp. 120-127, 2010.
- [2] J. Noble, C. A. Munro, V. S. Prasad, and R. Midha, "Analysis of upper and lower extremity peripheral nerve injuries in a population of patients with multiple injuries," Journal of Trauma and Acute Care Surgery, vol. 45, no. 1, pp. 116-122, 1998.
- [3] C. B. Novak, D. J. Anastakis, D. E. Beaton, S. E. Mackinnon, and J. Katz, "Relationships among pain disability, pain intensity, illness intrusiveness, and upper extremity disability in patients with traumatic peripheral nerve injury," The Journal of Hand Surgery, vol. 35, no. 10, pp. 1633-1639, 2010.
- [4] M. Ahmed-Labib, J. D. Golan, and L. Jacques, "Functional outcome of brachial plexus reconstruction after trauma," Neurosurgery, vol. 61, no. 5, pp. 1016-1023, 2007.
- [5] M. Siemionow and G. Brzezicki, "Current techniques and concepts in peripheral nerve repair," International Review of Neurobiology, vol. 87, pp. 141-172, 2009.
- J. W. Griffin, M. V. Hogan, A. B. Chhabra, and D. N. Deal, "Peripheral nerve repair and reconstruction," The Journal of Bone & Joint Surgery, vol. 95, no. 23, pp. 2144-2151, 2013.
- [7] M. T. Graham, N. von Guionneau, S. Tuffaha, and M. A. L. Bell, "Design and optimization of simulated light delivery systems for photoacoustic assessment of peripheral nerve injury," in Photons Plus Ultrasound: Imaging and Sensing, vol. 11960, pp. 275-281, SPIE, 2022.
- M. T. Graham, A. Sharma, W. M. Padovano, V. Suresh, A. Chiu, S. M. Thon, S. Tuffaha, and M. A. L. Bell, "Optical absorption spectra and corresponding in vivo photoacoustic visualization of exposed peripheral nerves," Journal of Biomedical Optics, vol. 28, no. 9, pp. 097001-097001, 2023.
- [9] A. Mallik and A. Weir, "Nerve conduction studies: essentials and pitfalls in practice," Journal of Neurology, Neurosurgery & Psychiatry, vol. 76, no. suppl 2, pp. ii23-ii31, 2005.
- [10] N. R. Holland, "Intraoperative electromyography," Journal of Clinical Neurophysiology, vol. 19, no. 5, pp. 444-453, 2002.

- [11] J. I. Suk, F. O. Walker, and M. S. Cartwright, "Ultrasonography of peripheral nerves," Current Neurology and Neuroscience Reports, vol. 13, no. 2, p. 328, 2013.
- [12] G. Rangavajla, N. Mokarram, N. Masoodzadehgan, S. B. Pai, and R. V. Bellamkonda, "Noninvasive imaging of peripheral nerves," Cells Tissues Organs, vol. 200, no. 1, pp. 69-77, 2015.
- [13] F. Toia, A. Gagliardo, S. D'Arpa, C. Gagliardo, G. Gagliardo, and A. Cordova, "Preoperative evaluation of peripheral nerve injuries: what is the place for ultrasound?," Journal of Neurosurgery, vol. 125, no. 3, pp. 603-614, 2016.
- C. M. Zaidman, M. J. Seelig, J. C. Baker, S. E. Mackinnon, and A. Pestronk, "Detection of peripheral nerve pathology: comparison of ultrasound and mri," Neurology, vol. 80, no. 18, pp. 1634-1640, 2013.
- [15] A. J. Cornelissen, T. J. van Mulken, C. Graupner, S. S. Qiu, X. H. Keuter, R. R. van der Hulst, and R. M. Schols, "Near-infrared fluorescence image-guidance in plastic surgery: a systematic review," European Journal of Plastic Surgery, vol. 41, pp. 269-278, 2018.
- [16] G. A. Throckmorton, E. Haugen, G. Thomas, P. Willmon, J. S. Baba, C. C. Solórzano, and A. Mahadevan-Jansen, "Label-free intraoperative nerve detection and visualization using ratiometric diffuse reflectance spectroscopy," *Scientific Reports*, vol. 13, no. 1, p. 7599, 2023. [17] P. Beard, "Biomedical photoacoustic imaging," *Interface Focus*, vol. 1,
- no. 4, pp. 602-631, 2011.
- [18] M. T. Graham, J. Y. Guo, and M. A. L. Bell, "Simultaneous visualization of nerves and blood vessels with multispectral photoacoustic imaging for intraoperative guidance of neurosurgeries," in Advanced Biomedical and Clinical Diagnostic and Surgical Guidance Systems XVII, vol. 10868, pp. 54-59, SPIE, 2019.
- [19] M. A. L. Bell, "Photoacoustic imaging for surgical guidance: principles, applications, and outlook," Journal of Applied Physics, vol. 128, no. 6, p. 060904, 2020.
- [20] R. Nachabé, J. W. van der Hoorn, R. van de Molengraaf, R. Lamerichs, J. Pikkemaat, C. F. Sio, B. H. Hendriks, and H. J. Sterenborg, "Validation of interventional fiber optic spectroscopy with mr spectroscopy, masnmr spectroscopy, high-performance thin-layer chromatography, and histopathology for accurate hepatic fat quantification," Investigative Radiology, vol. 47, no. 4, pp. 209-216, 2012.
- [21] P. Wang, H.-W. Wang, M. Sturek, and J.-X. Cheng, "Bond-selective imaging of deep tissue through the optical window between 1600 and 1850 nm," 2012.
- [22] J. M. Mari, W. Xia, S. J. West, and A. E. Desjardins, "Interventional multispectral photoacoustic imaging with a clinical ultrasound probe for discriminating nerves and tendons: an ex vivo pilot study," Journal of Biomedical Optics, vol. 20, no. 11, pp. 110503-110503, 2015.
- [23] R. Li, E. Phillips, P. Wang, C. J. Goergen, and J.-X. Cheng, "Labelfree in vivo imaging of peripheral nerve by multispectral photoacoustic tomography," Journal of Biophotonics, vol. 9, no. 1-2, pp. 124-128, 2016.
- A. D. Gaudet, P. G. Popovich, and M. S. Ramer, "Wallerian degenera-[24] tion: gaining perspective on inflammatory events after peripheral nerve injury," Journal of Neuroinflammation, vol. 8, no. 1, p. 110, 2011.